Published in final edited form as:
IEEE Trans Ultrason Ferroelectr Freq Control. 2011 November ; 58(11): 2281–2288. doi:10.1109/TUFFC.2011.2085

Novel PMN-PT free standing film for high frequency (80MHz) intravascular ultrasonic imaging

Xiang Li[1], **Qifa Zhou**[1], **K. Kirk Shung**[1], **Wei-Heng Shih**[2], and **Wan Y. Shih**[2]

[1]NIH Ultrasonic Transducer Resource Center and Department of Biomedical Engineering, University of Southern California, Los Angeles, California, 90089

[2]Department of Materials Science and Engineering, Drexel University, Philadelphia, PA 19104

Abstract

$[Pb(Mg_{1/3}Nb_{2/3})O_3]_{0.63}[PbTiO_3]_{0.37}$ (PMN-PT) free standing film of comparable piezoelectric property to bulk PMN-PT with a thickness of 33 μm has been fabricated using a modified precursor coating approach. At 1 KHz, the dielectric constant and loss were 4,160 and 0.0291, respectively. The remnant polarization and coercive field were 28 $\mu C/cm^2$ and 18.43 kV/cm. The electromechanical coupling coefficient k_t was measured to be 0.55, which was close to that of bulk PMN-PT single crystal material. A high frequency (80 MHz) miniature ultrasonic transducer with high sensitivity was fabricated from this film. In vitro imaging of a rabbit aorta was performed to demonstrate the application of this material to intravascular ultrasound imaging at 80 MHz. Compared to a 35 MHz ultrasonic image, the 80 MHz image showed superior resolution and contrast.

1. Introduction

Intravascular ultrasound (IVUS) has been proved to be a valuable medical imaging modality for the diagnosis of arterial diseases. The ability of directly imaging the vessel wall enables IVUS to provide more precise evaluations of lumen dimensions, plaque composition and calcium content.[1–4] A typical IVUS probe consists of a rotating shaft with a side-looking unfocused single element transducer, which leads to a radial imaging geometry of a cross section of a vessel. The size of an IVUS probe in clinical applications ranges from 2.6 to 3.5 french (0.90 – 1.17 mm), limiting the aperture of the transducer within the catheter to be less than 0.8 mm.[3] The center frequencies of commonly used IVUS transducers are between 20 to 50 MHz, implying that the axial/lateral resolutions are on the order of 60/200 μm. This value is inferior to intravascular Optical Coherence Tomography (OCT) imaging, of which the resolution is on the order of 10–30 μm, which could provide much more detailed information about the microstructures of vessel and plaque compositions. Its drawback is that it has a limited penetration depth of approximately 1 mm.[5–8] Increasing the IVUS center frequency to 80 MHz or higher is a compromise between resolution and penetration. To date, little IVUS work has been done at such a high frequency. The major concern is the strong tissue attenuation at high frequencies.[3] At 80 MHz, an attenuation coefficient of 10 dB/mm is expected for coronary artery, which means that a penetration depth of 3 mm can only be achieved for a system with a dynamic range of 60 dB. Yet such a system requires a highly sensitive miniaturized IVUS transducer, which is a great challenge.

The difficulty of such a high frequency transducer comes from preparation of a very thin layer of piezoelectric material with piezoelectric properties similar to bulk material. Traditional machining of bulk materials down to the thickness of 20–30 micrometers is extremely difficult and time-consuming. Additionally, quality deterioration and the brittle nature of the lapped bulk materials may severely downgrade the sensitivity of a high

frequency transducer. A more feasible solution is to pursue piezoelectric thin film technology. In our previous work, sol-gel lead zirconate titanate (PZT) and sputtered zinc oxide (ZnO) thin films have been investigated for fabrication of high frequency (>80 MHz) ultrasonic transducers.[9–11] However, the sensitivity of sol-gel PZT transducer was relatively low. The drawbacks to ZnO as active transducer elements are the low electromechanical coupling coefficient (k_t=0.28) and relative small dielectric constant($\varepsilon^r/\varepsilon_0$ =8), which make them not suitable for fabricating small aperture high sensitivity transducers.

PMN-PT thin films have been extensively studied (cite references). Due to the high k_t and $\varepsilon^r/\varepsilon_0$ values, it could be a good candidate for IVUS transducer fabrication. In this paper, we report the fabrication of novel PMN-PT freestanding thin films with enhanced piezoelectric properties. A highly sensitive miniaturized 80 MHz IVUS transducer was built from these films. In-vitro imaging of a rabbit aorta has been carried out to verify the feasibility of the transducer for intravascular imaging.

2. Fabrication and Characterization of PMN-PT Free Standing Film

$[Pb(Mg_{1/3}Nb_{2/3})O_3]_{0.63}[PbTiO_3]_{0.37}$ was synthesized using a modified precursor coating approach.[12] Nb_2O_5 (99.99%, Aldrich Chemical Co., Milwaukee, WI), titanium isopropoxide ($Ti(OCH(CH_3)_2)_4$, 99.9% Alfa Aesar), lead acetate anhydrous ($Pb(CH_3COO)_2.2Pb(OH)_2$, Fluka, St. Louis, MO), $Mg(Ac)_2.6H_2O$ (99.9%, Alfa Aesar), and NH_4OH (5M, Aldrich) were used in this study.

$Mg(Ac)_2.6H_2O$ (0.105 mol) was first dissolved in 500 mL of distilled water, followed by the addition of 0.1 mol of Nb_2O_5 powder to the solution. Ultrasonicated (50 MHz, 50 W, Ultrasonic Homogenizer 4710 series, Cole-Parmer Instrument Co., Vernon Hills, IL) was used for 10 min to break up the Nb_2O_5 agglomerates. To precipitate $Mg(OH)_2$ on to the Nb_2O_5 surface, NH_4OH (5M) was then continuous dropped into the suspension during this coating process to keep pH above 10.5 and kept stirring for 30 min. Then suspension was dried at 150°C using a hot plate. After drying, a precursor slurry was made from a lead acetate anhydrous ($Pb(CH_3COO)_2.2Pb(OH)_2$) solution in ethylene glycol (EG) ($HOCH_2CH_2OH$, Alfa Aesar, Ward Hill, MA) with 15% excess lead. The suspension was then dried at 230°C using a hot plate. Pyrochlore-free perovskite PMN powders was obtained by the dried PMN precursor powder, which was first heated at a rate of 1°C/min to 360°C for 2 h, followed by 5°C/min heating to 950°C for 2h.

A PT precursor solution in EG with a stoichiometric quantity of $Pb(CH_3COO)_2.2Pb(OH)_2$ and $Ti(OCH(CH_3)_2)_4$ were first prepared by dissolved in EG before mixing. The perovskite PMN powder was then suspended in a PT precursor solution containing lead acetate and titanium isopropoxide ($Ti(OCH(CH_3)_2)_4$, 99.9% Alfa Aesar) in EG and ball milled for 24 h. PMN-PT green powder was obtained by drying it on a hotplate at 230°C followed by heat treatment at a rate of 1°C/min to 360°C for 2h, which is ready for tape casting. The tape casting process was carried out by a tape casting company in Maryland.[13]

Sintering of PMN-PT green tape was done under controlled atmosphere because Pb is easy to evaporate at the sintering temperature which is usually higher than 1000°C. The green tape which had a thickness of 40 μm were cut to the size of 10 mm × 10 mm and placed on a flat alumina plate for sintering. To prevent the evaporation and loss of Pb element from PMN-PT tape during the sintering process at high temperature, 0.2 g of PbO powder (99.9%, Alfa Aesar) was placed in a small alumina crucible with a lid. Also another large alumina crucible was covered over both PbO powder crucible and PMN-PT green sheet to make the evaporated PbO to effectively contact PMN-PT sample to prevent Pb loss from the PMN-PT sample. The amount of evaporated PbO powder could be controlled by changing the crucible size and the opening of the lid. The typical evaporation of PbO was 20% of its

initial amount. To prevent the overexposure of the green sheet to the evaporated PbO, another crucible was covered over the green tape. Sintering temperature and time were 1,200°C and 2 hr, respectively.

The crystal phases of the sintered PMN-PT free standing film were characterized by X-ray diffractometry (XRD), shown in Fig. 1. The XRD pattern displayed a pure perovskite phase, indicating the film was well crystallized. The crystalline microstructures of the film were observed by scanning electron microscopy (SEM), shown in Fig. 2. The film was highly dense and without any crack or pore. The grain size was around 1–3 μm and film thickness was 33 μm. For the measurement of electrical properties, chrome/gold (Cr/Au) electrodes with dimension of 0.4×0.4 mm^2 were sputtered onto the film. The dielectric and ferroelectric properties were measured with an Agilent 4292A impedance analyzer (Agilent Technologies, Santa Clara, CA) and an RT6000 ferroelectric test system (Radiant Technology, Albuquerque, NM), respectively. The frequency dependence of the free relative dielectric constant ($\varepsilon^r/\varepsilon_0$) and the loss (tanδ) of the PMNPT film were measured from 1 KHz to 1 MHz, shown in Fig. 3. The $\varepsilon_r/\varepsilon_0$ and tanδ at 1 kHz were found to be 4160 and 0.0291, respectively. The $\varepsilon_r/\varepsilon_0$ value was higher than that reported by M. Kosec (4,100)[14], Danjela (3,600)[15], Hana (3,200)[16], M.L. Calzada (1,835)[17], lower than bulk material (5,229)[14]. The tanδ value was lower than those reported by M. Kosec (0.04)[14], Danjela (0.036)[15], M.L. Calzada (0.04)[17], and close to bulk material (0.02)[14]. The high relative permittivity and low loss of the PMN-PT free standing film imply a more optimized electrical impedance match and improved sensitivity for miniaturized high frequency transducers. The polarization-electric field hysteresis loop is shown in Fig. 4. The remnant polarization (P_r) and coercive field (E_c) were 28 μC/cm^2 (bulk, 12.3–33.1 μC/cm^2) [14] and 18.43 kV/cm (bulk, 3.3–4.3 kV/cm)[14], respectively. The saturation polarization (P_s) was around 46 μC/cm^2. After poling the material in DC electric field of 300kV/cm for 5 minutes at room temperature, the piezoelectric property was measured. The frequency dependence of the electrical impedance and phase are displayed in Fig. 5 which shows that the electrical impedance at resonant peak is 29 Ohm at 75 MHz, the series and parallel resonant frequency are 69 MHz and 80 MHz, and k_t is calculated to be 0.55 which is comparable to the bulk PMN-PT single crystal at 0.56 (HC materials, Bolingbrook, IL, USA).

3. Fabrication and Characterization of High Frequency Miniature Transducer

After characterization of the PMN-PT film, one piece of 7×10 mm^2 film was used as the active piezoelectric material to fabricate a side looking miniature transducer. The PMN-PT film was first sputtered with Cr/Au (500Å/1000Å) layers as electrodes at top and bottom. A matching layer made from Insulcast 501, sulcure 9 (American Safety Technologies, Roseland, NJ) and 2–3 μm silver particles (Sigma-Aldrich Inc., St. Louis, MO) was then cured over the top of the film and lapped to 5 μm. A conductive backing material, E-solder 3022 (VonRoll Isola, New Haven, CT) was applied to the bottom of the film and lapped to 0.6 mm. The active stack was diced along the thickness direction into small posts with the aperture of 0.4×0.4 mm^2. The post was housed within a 0.57-mm-ID polyimide tube (MedSource Technologies, Trenton, GA), on the side of which a window was opened to allow the transducer to slant toward side face. A 0.1-mm-OD electrical wire was connected to the conductive backing using E-solder 3022 inside the polyimide tube. The polyimide tube provided the electrical isolation from the outer stainless steel needle housing. The outer needle housing with an ID of 0.66 mm and OD of 0.92 mm had a window on the side for acoustic wave to go through. 5-min (??) epoxy was filled into the gap between piezoelectric post and needle housing to insulate the inner electrode. Another Cr/Au electrode was sputtered over the silver matching layer and stainless steel needle housing to form the ground connection. A 3-μm-thick parylene layer was vapor-deposited onto the aperture and

needle housing to serve as second matching and protecting layer. The transducer was finally connected to a brass holder and SMA connector for mechanical holding and electrical connection. To enhance the piezoelectric activity of the PMN-PT film, the finished transducer, shown in Fig. 6, was poled in a DC electric field of 300kV/cm for 5 minutes at room temperature.

The side looking miniature transducer's performance was measured in a de-ionized water bath at room temperature. Pulse-echo test[18] was conducted with an X-cut quartz as signal reflecting target. A single sinusoidal wave centered at 85 MHz with of approximately 100 Vpp and 200 Hz repetition rate emitted from a monocycle function generator (Avtech Electrosystems Ltd., Ontario, Canada) was used to excite the transducer. Echo signal was received and digitized by a 1 GHz oscilloscope (LC534, LeCroy Corp., Chestnut Ridge, NY). The frequency response of the transducer was analyzed from the echo waveform, shown in Fig. 7. The peak to peak amplitude was 601 mV. The measured center frequency was 84 MHz and −6dB fractional bandwidth was 35%. Two way insertion loss[18] was measured to be 25 dB, which indicated the transducer's sensitivity is comparable with that of a 80 MHz large aperture $LiNbO_3$ single crystal transducer (10–25 dB)[18]. Six-μm-diameter tungsten wire targets were imaged to determine axial and lateral resolutions of the transducer, as shown in Fig. 8(a). The envelopes of echo signals from the wire located at 1.2 mm away from the transducer surface, or Point Spread Function (PSF), were displayed in Fig. 8(b) and (c). The axial (Raxial) and lateral (Rlateral) resolutions were determined from the −6 dB envelope width, which were 35 μm and 176 μm, respectively.

4. In vitro Intravascular Imaging

In vitro imaging of a normal rabbit aorta was performed to test the transducer's ability for intravascular application. The side-looking PMNPT freestanding film transducer was used to image the cross section of an aorta, shown in Fig. 9(a). For comparison purpose, another image of the same aorta, but with a 35 MHz PMNPT-single-crystal needle transducer, which had the same aperture size (0.4×0.4 mm^2), shown in Fig. 9(b), was obtained. From these images, the 80 MHz PMNPT-Film transducer appeared to exhibit a much better resolution (denser speckles) than the 35 MHz PMNPT-single-crystal transducer. Due to the improved resolution, the vascular wall and the surrounding fatty tissues in the 80 MHz IVUS image were better differentiated than the 35 MHz image. Meanwhile, the 80 MHz IVUS could easily visualize the whole depth of vessel wall, though not the full depth of the hypoechoic fatty tissue. The 80 MHz image was depicted at a dynamic range of 51 dB and 35 MHz image was at 54 dB, implying 80 MHz freestanding film transducer had a comparable signal-to-noise ratio to the single crystal transducer.

5. Conclusions

In this paper, we utilized the piezoelectric thin film technology for high frequency (80MHz) IVUS application. The fabrication procedures of a high quality PMN-PT free standing thin film were presented. The measured dielectric and ferroelectric properties of the film were close to those of bulk material. Based on the film, a miniature side-looking IVUS transducer was fabricated and tested. Testing results showed the transducer had superior resolution and sensitivity. An in vitro study was conducted with a healthy rabbit aorta. The 80 MHz IVUS image demonstrated improved resolution and contrast to allow a differentiation of the vascular wall and surrounding fatty tissue, which could not be achieved by a 35 MHz transducer. As expected, the imaging depth in the hypoechoic fatty tissue was inferior to that of a 35 MHz transducer. However, this capability is especially attractive in detecting a vulnerable plaque consisting of a lipid pool surrounded by a fibrous cap given the improved

resolution and contrast at 80 MHz. A further increase in frequency will allow the resolution and contrast to be further improved by sacrificing the depth of penetration.

Acknowledgments

We would like to thank Mr. Jay Williams and Mr. Wei Wei for transducer fabrication and Ms. Jiechen Yin and Dr. Zhongping Chen for providing the tissue sample. This project has been supported by the NIH grants #P41-EB2182.

Refference

1. Potkin BN, Bartorelli AL, Gessert JM, Neville RF, Almagor Y. Coronary artery imaging with intravascular high-frequency ultrasound. Circulation. 1990; 81(5)
2. Nissen SE, Yock P. Intravascular ultrasound novel pathophysiological insights and current clinical applications. Circulation. 2001
3. Foster FS, Pavlin CJ, Harasiewicz KA, Christopher DA, Turnbull DH. Advances in ultrasound biomicroscopy. Ultrasound in Med & Biol. 2000; 26(1)
4. Prati F, Arbustini E, Labellarte A, Bello BD, Sommariva L, Mallus MT, Pagano A, Boccanelli A. Correlation between high frequency intravascular ultrasound and histomorphology in human coronary arteries. Heart. 2001; 85
5. Patwari P, Weissman NJ, Boppart SA, Jesser C, Stamper D, Fujimoto JG, Brezinski ME. Assessment of coronary plaque with optical coherence tomography and high-frequency ultrasound. The American Journal of Cardiology. 2000; 85
6. Brezinski ME, Tearney GJ, Weissman NJ, Boppart SA, Bouma BE, Hee MR, Weyman AE, Swanson EA, Southern JF, Fujimoto JG. Assessing atherosclerotic plaque morphology: comparison of optical coherence tomography and high frequency intravascular ultrasound. Heart. 1997; 77
7. Kawasaki M, Bouma BE, Bressner J, Houser SL, Nadkarni SK, MacNeill BD, Jang IK, Fujiwara H, Tearney GJ. Diagnostic accuracy of optical coherence tomography and integrated backscatter intravascular ultrasound images for tissue characterization of human coronary plaques. J Am Coll Cardiol. 2006; 48(1)
8. Sawada T, Shite J, Garcia-Garcia HM, Shinke T, Watanabe S, Otake H, Matsumoto D, Tanino Y, Ogasawara D, Kawamori H, Kato H, Miyoshi N, Yokoyama M, Serruys PW, Hirata K. Feasibility of combined use of intravascular ultrasound radiofrequency data analysis and optical coherence tomography for detecting thin-cap fibroatheroma. Eur Heart J. 2008; 29(9)
9. Cannata JM, Williams JA, Zhou QF, Sun L, Shung KK, Yu H, Kim ES. Self-focused ZnO transducers for ultrasonic biomicroscopy. Journal of Applied Physics. 2008; 103
10. Zhu BP, Wu DW, Zhou QF, Shi J, Shung KK. Lead zirconate titanate thick film with enhanced electrical properties for high frequency transducer applications. Applied Physics Letters. 2008; 93
11. Zhu BP, Zhou QF, Shi J, Shung KK, Irisawa S, Takeuchi S. Self-separated hydrothermal lead zirconate titanate thick films for high frequency transducer applications. Applied Physics Letters. 2009; 94
12. Luo H, Shih WY, Shih W-H. Double Precursor Solution Coating Approach for Low-Temperature Sintering of Sintering of $[Pb(Mg_{1/3}Nb_{2/3})O_3]0.63[PbTiO_3]0.37$ Solids. J Am Ceram Soc. 2007; 90(12):3825–3829.
13. Maryland Ceramic & Steatite Co., Inc. 3100 Dublin Road Street, MD 21154:
14. Kosec M, Holc J, Kuscer D, Drnovšek S. $Pb(Mg_{1/3}Nb_{2/3})O_3$-$PbTiO_3$ thick films for mechanochemically synthesized powder. Journal of the European Ceramic Society. 2007; 27
15. Kuščer D, Skalar M, Holc J, Kosec M. Processing and properties of $0.65Pb(Mg_{1/3}Nb_{2/3})O_3$–$0.35PbTiO_3$ thick films. Journal of the European Ceramic Society. 2009; 29
16. Uršič H, Škarabot M, Hrovat M, Holc J, Skalar Miha, Bobnar V, Kosec M, Muševič I. The electrostrictive effect in ferroelectric $0.65Pb(Mg_{1/3}Nb_{2/3})O_3$–$0.35PbTiO_3$ thick films. Journal of Applied Physics. 2008; 103
17. Calzada ML, Alguero M, Ricote J, Santos A, Pardo L. Preliminary results on sol-gel processing of <100> oriented $Pb(Mg_{1/3}Nb_{2/3})O_3$–$PbTiO_3$ thin films using diol-based solutions. J Sol-Gel Sci Techn. 2007; 42

18. Cannata JM, Ritter TA, Chen WH, Silverman RH, Shung KK. Design of efficient, broadband single-element (20–80 MHz) ultrasonic transducers for medical imaging applications. IEEE Transactions on Ultrasonics Ferroelectrics and Frequency Control. 2003; 50(11)

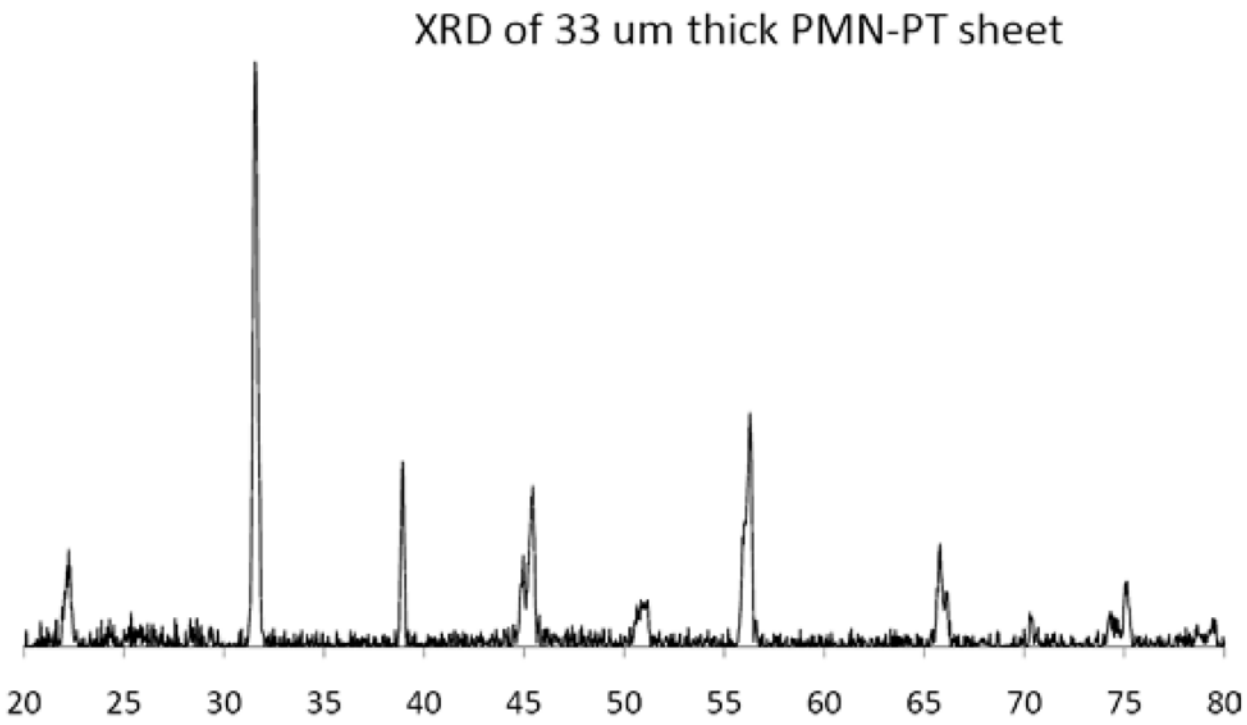

Fig. 1.
X-ray diffraction(XRD) pattern of the PMN-PT free standing film

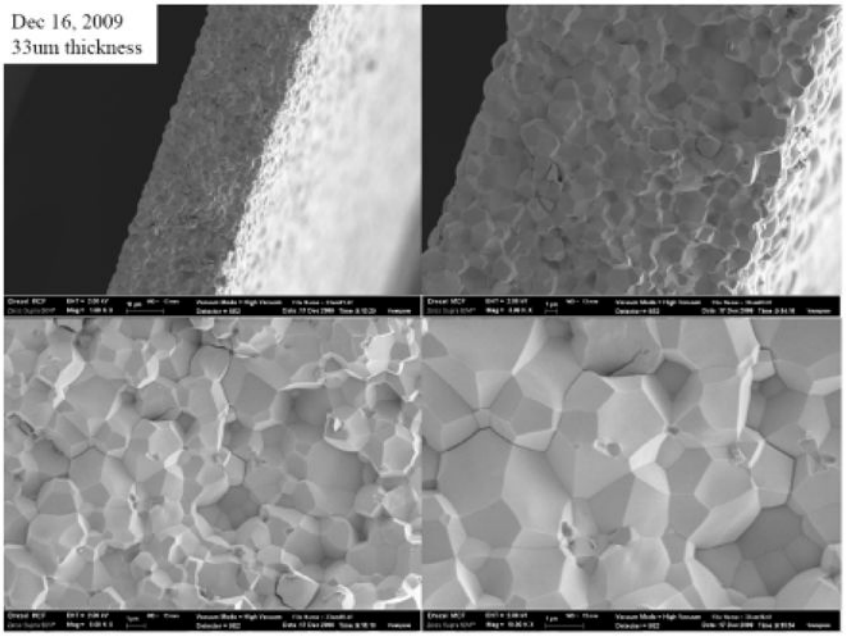

Fig. 2.
SEM micrograph of the PMN-PT free standing film

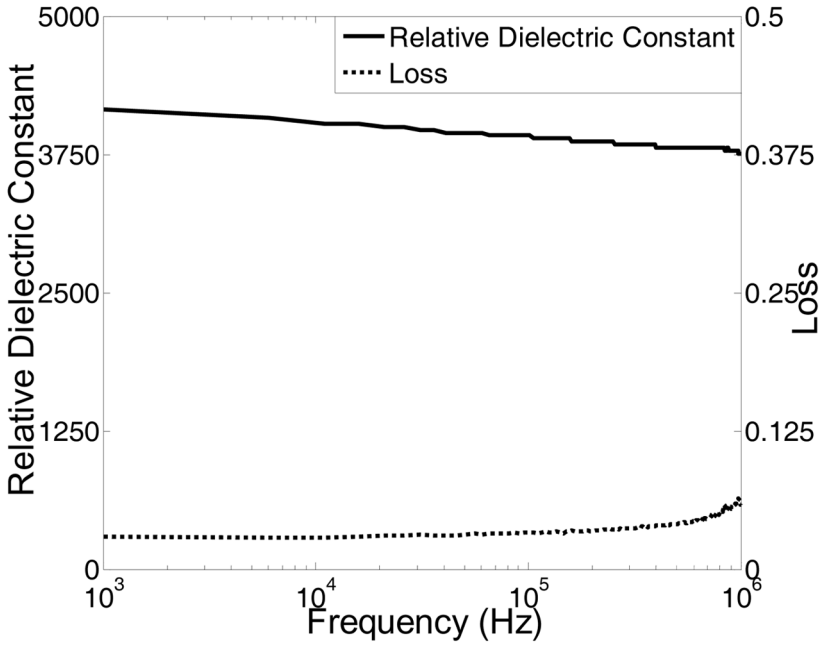

Fig.3.
Frequency dependence of dielectric constant (solid line) and loss (dashed line) for PMNPT film.

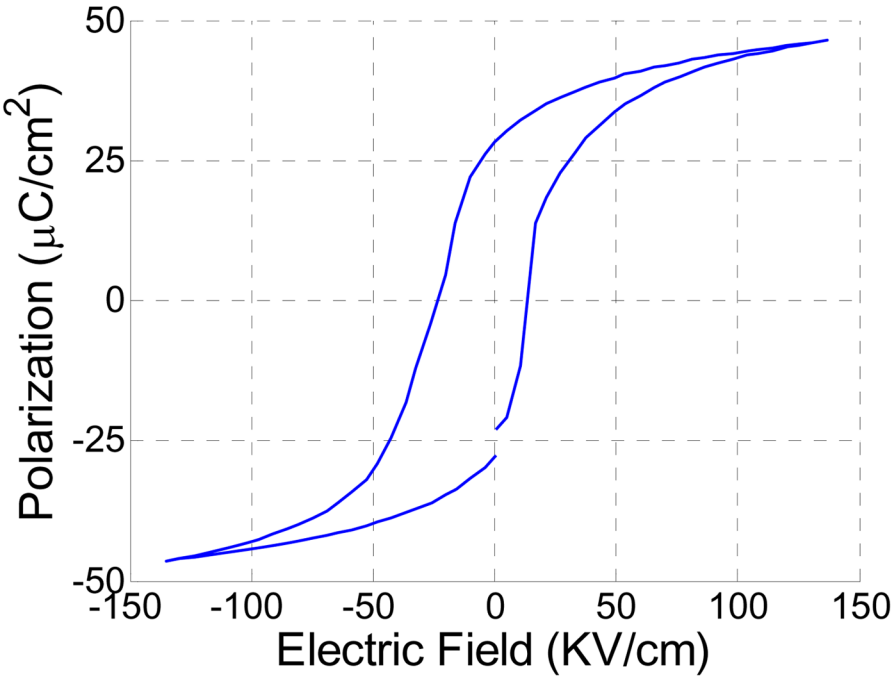

Fig. 4.
Polarization-electric field hysteresis loop of the annealed PMNPT film

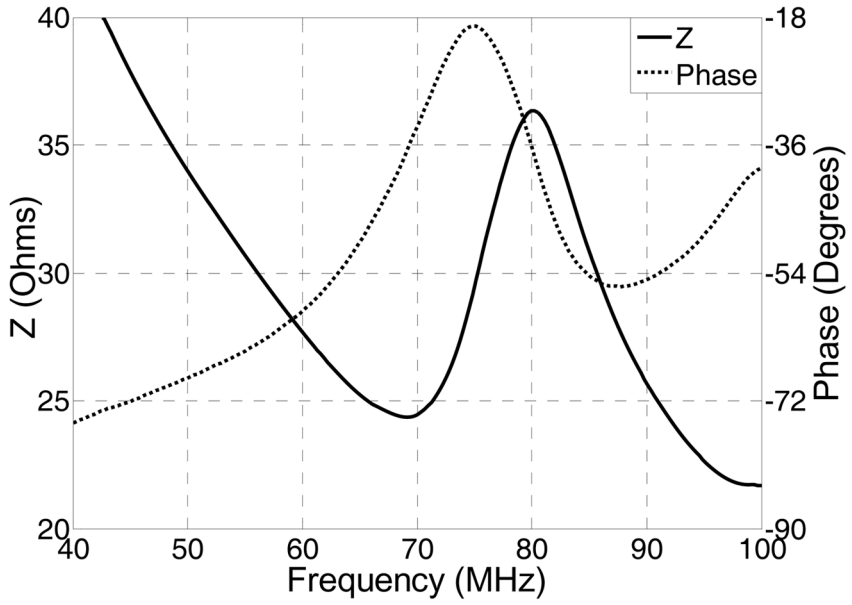

Fig. 5.
Electrical impedance of PMNPT film

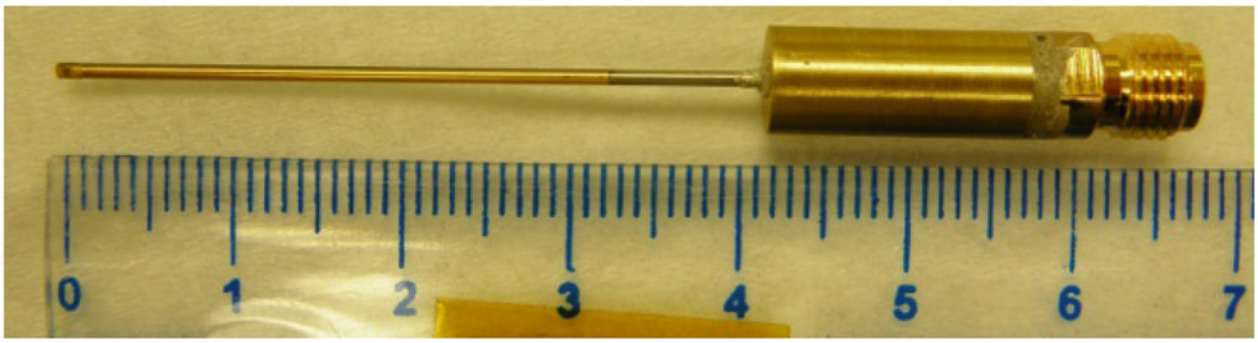

Fig. 6.
side-looking miniature transducer

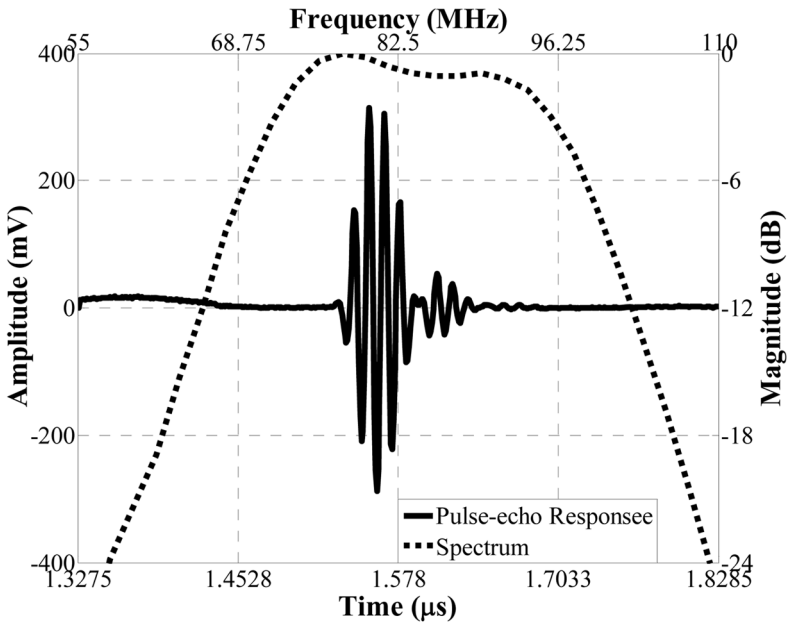

Fig. 7.
Pulse-echo measurement of one representative transducer

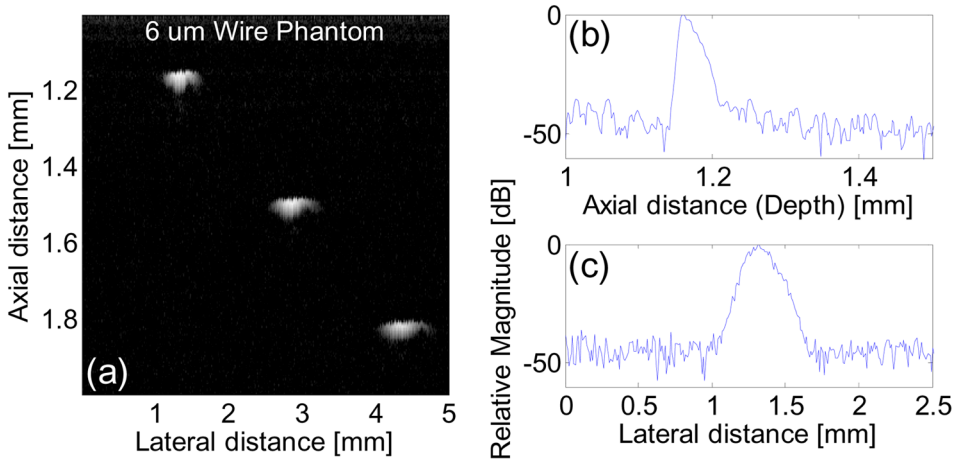

Fig. 8.

Ultrasound wire phantom (a), displayed with a dynamic range of 45 dB; axial (b) and lateral (c) envelopes of echo signals from the wire located at 1.2 mm away from the transducer surface

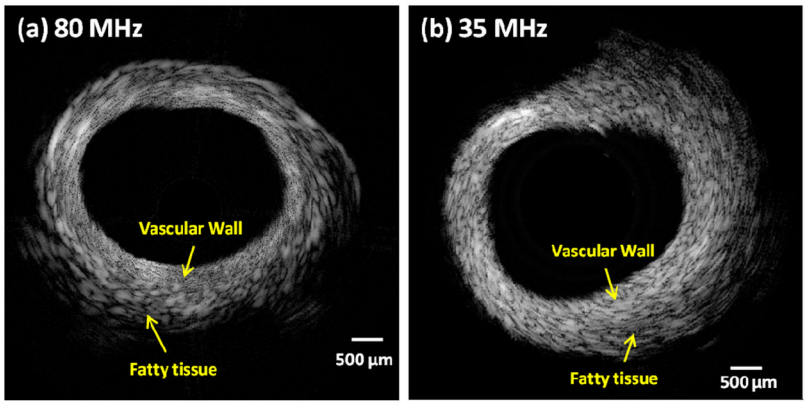

Fig. 9.

(a) Rabbit aorta image from 80-MHz PMNPT-freestanding-film transducer; (b) The same aorta image from 35-MHz PMNPT-single-crystal transducer.